Scientific African 8 (2020) e00298

Contents lists available at ScienceDirect

Scientific African

journal homepage: www.elsevier.com/locate/sciaf

# Computational modelling and simulation of the feasibility of a novel dual purpose solar chimney for power generation and passive ventilation in buildings

Abayomi T. Layeni[a,c,*], M. Adekojo Waheed[b], Babatunde A. Adewumi[b], Bukola O. Bolaji[d], Collins N. Nwaokocha[a,*], Solomon. O Giwa[a]

[a] Department of Mechanical Engineering, Olabisi Onabanjo University, Ago-Iwoye, Nigeria
[b] Department of Mechanical Engineering, Federal University of Agriculture, Abeokuta, Nigeria
[c] School of Engineering, University of the West of Scotland, Paisley Campus, Scotland
[d] Department of Mechanical Engineering, Federal University, Oye-Ekiti, Nigeria

ARTICLE INFO

*Article history:*
Received 18 January 2019
Revised 18 December 2019
Accepted 26 January 2020

Editor: Dr. B. Gyampoh

*Keywords:*
Building
Solar chimney
Stack effect
CFD
ANSYS

ABSTRACT

This paper presents numerical study and analysis of a novel application of a proposed solar chimney system to help solve the problem of ventilation (thermal comfort) and energy management (inadequate power supply) of buildings in the tropics. The main objective of the study is to determine the feasibility of the proposed system vis-à-vis the airflow rate within the room for adequate ventilation and within the solar chimney for required velocity to power a small size wind turbine. The commercial Computational Fluid Dynamics package FLUENT (ANSYS WORKBENCH 14.5) was used for the simulation. The computational domain consist of a 2-D 4 × 4 $m^2$ room and solar chimney with varying heights between 5 and 9 m and gap between 0.5 and 1 m. The solar radiation condition with solar heat flux (SHF) of between 200 and 1,000 $W/m^2$ and ambient wind conditions of no wind and wind speed of 1.0 to 8.0 m/s were simulated. The validation of simulated results with experimental data from previous studies showed conformity with a deviation not more than 2.5%. Results showed that the room mass flow rate increased from 1.0 kg/s with no wind effect to about 30.1 kg/s with induced wind of 1.0 to 8.0 m/s. The air mass flow rate increased from about 0.57 to 0.91 kg/s at chimney height of 5 and 9 m respectively for no wind condition and SHF of 400 $W/m^2$. The power outputs obtained from the SC with SHF of 400 $W/m^2$ for chimney height of 5 and 9 m were 32.8 and 85.2 $W/m^2$ respectively. The results presented helps layout and establish the fundamentals and system response to temperature and airflow of a solar chimney system used for the combined purpose of passive ventilation and power generation in a building.



* Corresponding author.
*E-mail addresses:* yomilayeni@gmail.com (A.T. Layeni), collinsnwaokocha@gmail.com (C.N. Nwaokocha).

https://doi.org/10.1016/j.sciaf.2020.e00298

## Introduction

The present state of technology of using the solar chimney for two different purposes (either for power generation or for ventilation) have been researched by various researchers [15,21,27,29,38]. However, this research attempts to model a system that will combine the dual purpose of the Solar Chimney (SC) as one system. Such system will not only help in reducing the global greenhouse emission, but will also be a means of reducing the energy cost of a household and will be a step further in achieving the eco-friendly habitation.

Schlaich and Schiel, [40] stated that practical solar energy technology should be simple, reliable and within the reach of less developed countries. A device that should not require cooling fluids or generate waste heat, and be based on renewable materials. The solar chimney technology satisfy the above mentioned criteria and a step further towards a worldwide solar energy dependent economy. It is reported that even low rated solar chimneys (100 and 200 MW) are capable of generating power at comparable costs to those of conventional power generating plants [40]. This is a good reason for the development of this solar energy system on a large scale, which will help promote economic and environmentally suitable exploitation of energy in sunny regions in the future.

The concept of the novel solar chimney here presented is the application of the solar chimney system in the regions of the world with solar radiant temperatures high enough for the development of the solar chimney power plant coupled with the ventilation solar chimney using the stack effect induced in the chimney in ventilating adjourning room(s). And as such, address issues with inadequate power supply and thermal discomforts of high temperature and humidity in tropical regions and less developed countries.

Schlaich and Schiel [40] and Nouanégué and Bilgen [32] noted various uses of chimneys for purposes such as heating and ventilating of buildings, drying of agricultural produce, and for other passive systems [6,9,14].

The Solar Chimney (SC) ventilation system is different from a traditional chimney as at least one of its walls is made of transparent material, which allows solar radiation into the chimney. As the chimney wall heats up, the air temperature inside the SC channel increases due to heat transfer from the walls and the buoyancy effect thus created drives the airflow through the channel. The pressure difference between the SC and the adjoining building draws air from the interior of the building, through the SC and out of the system. The air is then replaced by fresh air sucked into the building through openings, accomplishing natural ventilation. The induced ventilation flowrates and air temperature in the chimney are important performance indicators of the SC.

The Trombe wall is also used as solar chimney for building ventilation. Lal et al. [23] suggested that some alterations with flow control arrangement and combination methods with some other types of passive systems are possible. Trombe wall, developed as solar chimney system by Trombe and Michel, is a type of passive solar heating system for buildings [3]. The Trombe wall was used by Bansal et al. [4] for building ventilation and a mathematical model was developed for calculating the air change per hour (ACH) of the system. Heat transfer models of the SC for building ventilation analysis was developed by Ong [34] while an experimental study was carried out by Ong and Chow [35]. Bouchair et al. [11] and Bouchair [10] carried out studies on optimising the SC width for maximum airflow. Gan and Riffat [18] studied a simple SC for passive ventilation and with heat recovery system for buildings using CFD techniques, where investigation for improved performance was carried out based on the ventilation rate, solar heat gain and glazing type. Observations made show that the double or triple glazed SC wall material gave better ventilation effect than single glazed chimney. Additional parametric study on the Trombe wall by Gan [16,17] for the purpose of passive cooling of buildings was carried out, where flow equations were developed for computing the mass flowrate, the effect of heat gain on wall, and the heat storage height of chimney on air flowrate for certain conditions.

As noted by Schlaich and Schiel [40], three essential elements of the solar chimney power generation plant are the glass collector, chimney, and turbines. A solar chimney power plant combines these elements in a novel way [24,37,40,43]. In the collector, solar heat flux heats up an absorber (ordinarily soil or water bags) on the ground, the absorber then heats up a large body of air, which rises up the chimney, due to density difference of air between the chimney base and the environs. As the air rises from the base through the SC, it drives turbines connected at the chimney base to generate electricity. The concept of solar chimney power generation technology was conceived many years ago and first described in a publication by Gunther in 1931 ([45]a), which was presented again in 1978 and demonstrated with the operation of a 50 kW pilot power plant in Manzanares, Spain ([43]b).

Zhou et al. [43] made observations with respect to the prototype built in Manzanares that the output power of 102.2 kW was obtained for an optimal chimney height of 615 m. however, this output power was obtained at a height lower than the maximum chimney height of 788 m with gave an output power of 92.3 kW. Sensitivity analyses performed to show the effect of lapse rates of atmospheric temperatures and solar collector radii on maximum chimney height indicated that the maximum height steadily increases as the lapse rate increases and go to infinity at around 0.0098 Km, and that power output increase with larger solar collector radius.

Pretorius and Kröger [39] presented results indicating that windy conditions may negatively affect plant performance significantly, while night-time temperature inversions cause major reductions in night-time output.

Chen and Li [12] established that an optimum air gap to height ratio exist and noted that it is a function of the chimney inlet conditions. The effect of ventilation on air change in a school building in Thailand was studied by Khedari et al. [22]. The results obtained show that the number of air change rate varied between 8 – 15 and temperature reduced by 2 – 3 °C. Simulations by Barozzi et al. [5] investigated air movement in a model building and observed a good agreement between

simulation and experimental results. Awbi and Gan [2] also carried out simulations studies on a solar chimney. Results obtained also show good agreement with simulated results of other researchers and Bouchair's [10] experimental results.

Zalewski et al. [41] carried out simulation studies validated by experimental results using TRANSYS to model and analyse a SC. The results obtained show better energy performance for composite walls than classical wall in cool weather conditions. Lipping and Angui [26] carried out studies to test the reliability and accuracy of the $k-\varepsilon$ turbulence model on a SC. They recommended that an air gap - chimney height ratio of about 0.5 will perform optimally and minimum chimney height greater than $1m$ be used for vertical collector.

Bachoroudis et al. [3] carried out numerical studies to investigate the flow field and heat transfer of natural convection phenomena inside a solar chimney. The results obtained noted that the $k-\varepsilon$ turbulence model provides better performance than other flow models for boundary layers with strong adverse pressure gradient. Nouanegue et al. [31] stated that other parameters, like Rayleigh number (Ra), Reynold number (Re), aspect ratio, exit size ($h/L$) and wall thickness, affects the performance of a SC. Bassiouny and Koura [7,8] carried out theoretical and computational studies of SC systems for improving natural ventilation in Egypt. Bassiouny and Koura [7,8] developed an optimised model of the chimney inclination angle using FORTRAN programme, which resulted to be in the range of $45^{O}$ to $70^{O}$ for the location of latitude 28.4° with chimney width in the range of 0.1 to $0.35m$ and solar heat flux of $500W/m^2$.

Zamora and Kaiser [42] carried out computational study of free convection in SC. The Reynolds $k-\omega$ turbulence model was used for simulation of a range of Rayleigh number ($10^5$ to $10^{12}$) with symmetrical isothermal heating. Gan [16] developed a heat transfer rate and airflow rate correlation models for analysis using Nusselt number, Reynolds number and Rayleigh number as variables in ventilation area for a given SC height and width. Hughes and Ghani [19] carried out the simulation studies for the feasibility of wind-vent. Simulations were conducted using Computational fluid dynamics software (FLUENT). They investigated the effect of the utilisation of mechanical pressure by fans to attain minimum natural ventilation during low ambient wind velocity. They noted that locating the fan at the bottom side gave the maximum ventilation rate in comparison to the middle and top locations of the wind-vent.

## Present study

The present state of technology of using the Solar Chimney for two different purposes (that is for power generation and for ventilation) have been explored by various researchers; however, this research attempts to combine these purposes into one system, a system that will combine the dual purpose of the Solar Chimney as one unified system. This study presents an alternative methodology and analysis of the study of Layeni et al. [25] on the combined ventilation and power solar chimney. Such system will not only help in reducing the global greenhouse emission, but will also be a means of reducing the energy cost of a household and will be a step further in achieving the Eco-friendly habitation. The research presents the use of CFD for the study of novelty solar chimney for combined ventilation and power in buildings. The redesigned SC is very effective in building to achieving the high level of energy management and green environment status for sustainable development. Energy demand for ventilation and other purposes in residential and commercial buildings can be reduced to a large extent with the additional power generated from the system. The research is on-going and various modifications are being studied to improving the performance of the system, develop a prototype and standardising the solar chimney system for residential and commercial buildings.

The study is justified as there are many regions of the earth the solar radiant insolation and temperatures are high enough for the development of the solar chimney systems. The outcome of research will help in establishing the basic models for the design and development of the novel concept of dual purpose SC for ventilation and power generation. Thus, developing systems that can be environmentally friendly in the context of the green environment and sustainable development, as it will aid in reducing the overall household energy cost and production of greenhouse gasses.

### *The model*

Physical systems are represented as models to enable thorough analysis of the response of the systems in operating conditions and a means of predicting the behaviour of the system under other desired conditions. The results of the analysis will help to developing a better understanding and implementation of the SC model in buildings and the development of SC retrofit for existing buildings for passive ventilation and power generation.

The atmospheric condition for this study was based on a location in South-west Nigeria, with ambient average temperature of 27° C, mean air velocity of 1.2 m/s, atmospheric pressure of 1013mb [20], and the mean solar radiation of about 200 W/m$^2$ [33]. The set-up of physical model is as shown in Fig. 1, in which the Combined Solar Chimney consists of a horizontal Solar Collector section and a vertical Solar Collector (Chimney) section with glass as wall material of the section facing the Sun. Solar energy enters through the glass wall and heats up air inside the horizontal Solar Collector and vertical Solar Chimney. The following are assumptions made in the analysis [28]:

1. Steady state heat transfer is assumed with the solar heat flux and the ambient mean temperature constant;
2. Turbulent air flow is assumed inside the chimney;
3. The system is frictionless and void of leakages;
4. Boussinesq approximation is assumed with all physical properties of air meeting this condition and only the buoyancy force is considered;

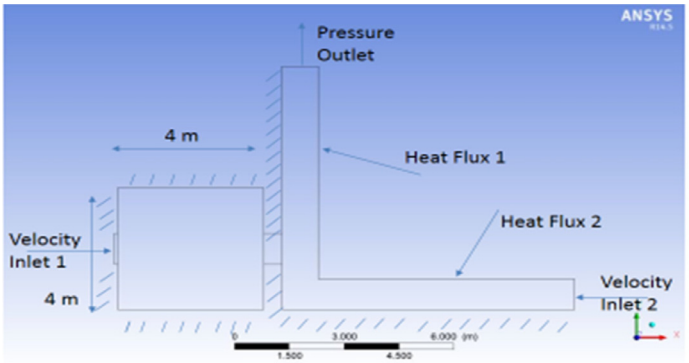


**Fig. 1.** Physical model.

**Table 1**
Nomenclature

| | | | |
|---|---|---|---|
| $C$ | Constant | $T$ | Temperature |
| $C_p$ | Specific heat | $t$ | Turbulence |
| $f_p$ | Buoyancy force | $U$ | Velocity |
| $g$ | Gravitational constant | $\alpha$ | Absorptivity |
| $h$ | Enthalpy | $\beta$ | Coefficient of thermal expansion |
| $k$ | Kinetic energy | $\varepsilon$ | Energy dissipation |
| $keff$ | Effective conductivity | $\mu$ | Dynamic viscosity |
| $k_f$ | Fluid thermal conductivity | $\mu_t$ | Turbulent viscosity |
| $k_t$ | Turbulent thermal conductivity | $\rho$ | Density of air |
| $p$ | Pressure | $\rho_0$ | Reference density |
| $prt$ | Turbulent Prandtl number | $\sigma$ | Compressive stress |
| $s_h$ | Source term with solar radiation | | |

**Table 2**
Dimensions of modelled solar chimney.

| S.No. | Specifications | Dimensions ($m$) |
|---|---|---|
| 1. | Dimension of room | 4 × 4 |
| 2. | Air gap between glazing and wall | 0.5 – 1.0 |
| 3. | Chimney height | 5 – 9 |
| 4. | Dimension of horizontal solar collector (inlet vent) | 8 × 1 |
| 5. | Dimension of room inlet vent | 1 |

5. Infiltrating flow of air through the chimney wall is neglected;
6. The temperature of the ground under the heat insulator bed is assumed equal to that of the ambient.

## CFD simulation strategy

The steady state $k-\varepsilon$ turbulence model, with the Reynolds-Averaged Navier-Stokes equations (RANS) are used for modelling. The air density variation in the buoyancy flow is accounted for by the Bousinesq approximation. The dimensions of the simulated 2D solar chimney model are shown in Table 2.

All simulations were based on the $k-\varepsilon$ turbulence model and the basic equation summarised as below.

### *Basic equations*

The CFD analysis of this study is performed using ANSYS FLUENT software. The mathematical model for the CFD analysis are the Navier-Stokes equations (the Continuity and momentum equations), the energy and state equations for the heat transfer analysis of the system. Additional transport equations are modelled for turbulent flow [1].

The solution variables in the instantaneous Navier-Stokes equations using Reynolds averaging, are decomposed into the mean (ensemble-averaged) and fluctuating components. For the velocity components Eqn. (1):

$$u_i = \hat{u}_i + u_i' \tag{1}$$

where $\bar{u}_i'$ and $u_i'$ are the mean and fluctuating velocity components ($i = 1, 2, 3$).

Similarly, for pressure and other scalar quantities Eqn. (2):

$$\phi = \hat{\phi}_i + \phi' \tag{2}$$

where $\phi$ represents a scalar quantity such as pressure and energy.

Substituting equations of the flow variables into the equations for instantaneous continuity and momentum and taking a time average yields the ensemble-averaged momentum equations. Written in Cartesian tensor form as:

$$\frac{\partial \rho}{\partial t} + \frac{\partial}{\partial x_i}(\rho u_i) = 0 \tag{3}$$

$$\frac{\partial}{\partial t}(\rho u_i) + \frac{\partial}{\partial x_j}\left(\rho u_i u_j\right) = -\frac{\partial}{\partial x_i} + \frac{\partial}{\partial x_j}\left[\mu\left(\frac{\partial u_i}{\partial x_j} + \frac{\partial u_j}{\partial x_i} - \frac{2}{3}\delta_{ij}\frac{\partial u_l}{\partial x_l}\right)\right] \tag{4}$$

Eqs. (3) and (4) are the Reynolds-averaged Navier-Stokes (RANS) equations, which is of the same form as the instantaneous Navier-Stokes equations. The time-averaged values of the velocities and other solution variables represented. Added terms appearing represents turbulence effects. Modelled Reynolds stresses $(-\rho\overline{u_i' u_j'})$ are used to close Eq. (4).

A requirement by the Reynolds-averaged approach to turbulence modelling is that in the Boussinesq hypothesis the Reynolds stresses and the mean velocity gradients are modelled as Eqn. (5):

$$-\rho\overline{u_i' u_j'} = \mu_t\left(\frac{\partial u_i}{\partial x_j} + \frac{\partial u_j}{\partial x_i}\right) - \frac{2}{3}\left(\rho k + \mu_t \frac{\partial u_k}{\partial x_k}\right)\delta_{ij} \tag{5}$$

The Boussinesq hypothesis is used in the $k$ – $\varepsilon$ models, which is employed in the study. (Peri et al., [36]) All the simulations of the air flow use the $k$ – $\varepsilon$ turbulence model. The model transport equations for the turbulence kinetic energy ($k$) and the kinetic energy dissipation rate ($\varepsilon$) is used to develop a semi-empirical model of the standard $k$ – $\varepsilon$ model as

$$\frac{\partial}{\partial t}(\rho k) + \frac{\partial}{\partial x_i}(\rho k u_i) = \frac{\partial}{\partial x_j}\left(\left(\mu + \frac{\mu_t}{\sigma_k}\right)\frac{\partial k}{\partial x_j}\right) + G_k + G_b - \rho\varepsilon + S_k \tag{6}$$

$$\frac{\partial}{\partial t}(\rho \varepsilon) + \frac{\partial}{\partial x_i}(\rho \varepsilon u_i) = \frac{\partial}{\partial x_j}\left(\left(\mu + \frac{\mu_t}{\sigma_\varepsilon}\right)\frac{\partial \varepsilon}{\partial x_j}\right) + C_{l\varepsilon}(G_k + C_{3\varepsilon}G_b) - C_{2\varepsilon}\rho\frac{\varepsilon^2}{k} + S_\varepsilon \tag{7}$$

In the Eqs. (6) and (7) above, $G_k$ represents generation of turbulence kinetic energy due to mean velocity gradients, and $G_b$ represents generation of turbulence kinetic energy due to buoyancy.

ANSYS FLUENT solves the energy equation in the following form:

$$\frac{\partial}{\partial t}(\rho E) + \nabla \cdot \left(\vec{V}(\rho E + \rho)\right) = \nabla \cdot \left(k_{eff}\nabla T - \sum_J h_j \vec{j}_j + \left(\bar{\tau}_{eff} \cdot \vec{V}\right)\right) + S_h \tag{8}$$

Where $k_{eff}$ is the effective conductivity given by $k + k_t$, where $k_t$ is the turbulent thermal conductivity, and $\vec{j}_j$ is the diffusion flux of species $j$. The energy transfer due to conduction, species diffusion, and viscous dissipation are the first three terms on the right-hand side of Eq. (8) respectively. $S_h$ includes the heat of chemical reaction, and any other volumetric heat sources defined.

In Eq. (9)

$$E = h - \frac{P}{\rho} + \frac{v^2}{2} \tag{9}$$

Where sensible enthalpy $h$ is defined for ideal gases as Eqn. (10)

$$h = \sum_j Y_j h_j \tag{10}$$

and for incompressible flow as Eqn. (11)

$$h = \sum_j Y_j h_j + \frac{p}{\rho} \tag{11}$$

*Buoyancy-driven and free convection flow theory*

The addition of heat to a fluid results in density variation with respect to temperature, which may induce a flow due to the force of gravity acting on the density variations. Buoyancy-driven flows, also known as natural convection (or mixed-convection) flows, can be modelled by ANSYS FLUENT. The significance of buoyancy forces in a mixed convection flow can be measured by the ratio of the Grashof and Reynolds numbers Eqn. (12):

$$\frac{Gr}{Re^2} = \frac{g\beta\Delta TL}{v^2} \tag{12}$$

**Table 3**
Properties of materials.

| Material | $\rho$, kg/m$^3$ | $C_p$, j/kg°C | k, W/m°C |
|---|---|---|---|
| Glass | 2500 | 800 | 0.8 |
| Air | 1.225 | 1006.43 | 0.0242 |

**Table 4**
Molecular weight and viscosity of air.

| Property | Value |
|---|---|
| Viscosity (kg/ m-s) | $1.7894 \times 10^{-5}$ |
| Molecular weight (kg/kmol) | 1.225 |

**Table 5**
Grid refinement.

| GRID | Nodes | Elements | Nusselt Number (NU) | % Difference |
|---|---|---|---|---|
| **1** | 208 | 159 | 108.94 | |
| **2** | 215 | 166 | 110.84 | 1.8919 |
| **3** | 322 | 260 | 108.93 | 1.9068 |
| **4** | 321 | 358 | 109.92 | 0.9943 |
| **5** | 825 | 720 | 109.92 | 0 |

When this ratio is close to or exceeds unity, strong buoyancy contributions to the flow is expected. Conversely, if this ratio is very small, buoyancy forces may be ignored in the simulation. In pure natural convection, the intensity of the buoyancy-induced flow is measured by the Rayleigh number Eqn. (13):

$$Ra = \frac{g\beta \Delta T L^3 \rho}{\mu \alpha} \tag{13}$$

Where $\beta$ is the thermal expansivity Eqn. (14):

$$\beta = -\frac{1}{\rho}\left(\frac{\partial \rho}{\partial T}\right)_p \tag{14}$$

And $\alpha$ is the thermal diffusivity Eqn. (15):

$$\alpha = \frac{k}{\rho c_p} \tag{15}$$

*Boundary conditions*

A static pressure boundary condition is used at chimney exit, which implies that pressure at inlet and outlet of SC is equal to the atmospheric pressure. And the simulated inlet temperature of SC is equal to the room temperature. A static pressure boundary condition is also used at the room and horizontal solar collector inlets except when simulating the effect of wind on the system. The power generated has been simulated and analysed as power generation from a wind turbine. The solar radiation and ambient wind simulated are 200 – 1,000 W/m$^2$ and 0.05 -

*Main input parameters*

Important properties of materials and modelling parameters used for simulation are shown in Table 3 below. The molecular weight and viscosity of air is presented in Table. 4.

## Verification of model

ANSYS workbench 14.5 was used to develop a two Dimensional (2D) model. Grid quality plays a significant role on the quality of the analysis, regardless of the flow solver used. Convergence and accuracy of CFD solutions relies on the mesh quality. The numerical model was verified taking values of the response Nu for different grid refinements: for grid with 208 nodes and 159 elements the value of Nu was 108.94 and for grid with 825 nodes and 720 elements the Nu was 109.92. It was observed that the sensitivity of grid refinement became negligible from Nu of a grid size of 321 nodes and 358 elements (Table 5).

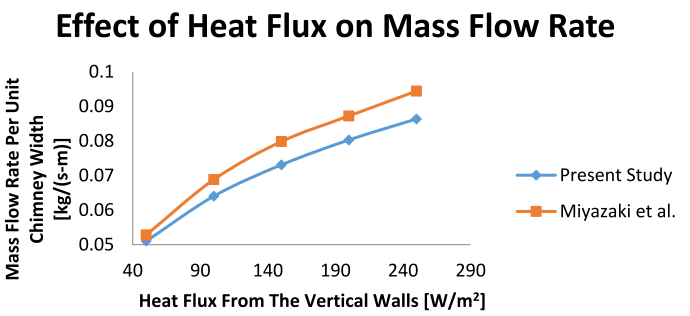


**Fig. 2.** The effect of heat flux on mass flow rate of the present study in comparison with CFD results from Miyazaki et al. [30]

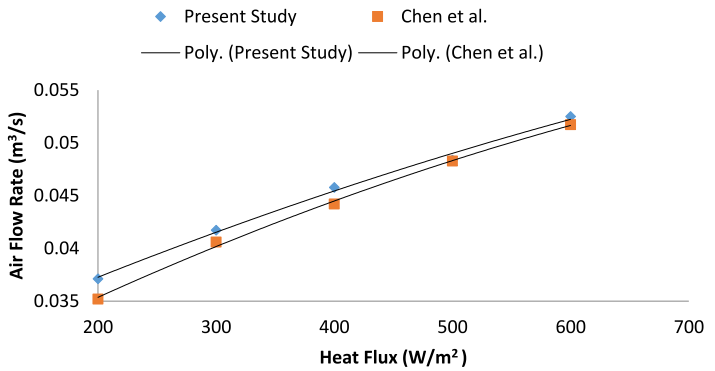


**Fig. 3.** Comparison of the present simulated airflow rate through the chimney with 200 mm gap with experimental results from Chen et al. [13] at different input solar heat flux.

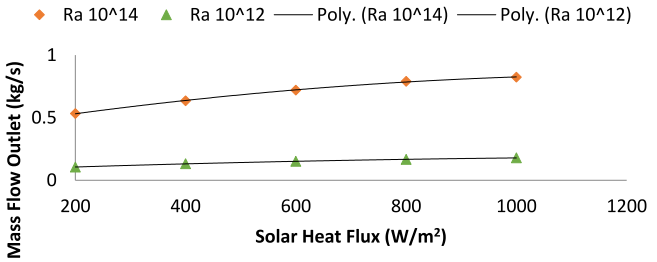


**Fig. 4.** The effect of solar heat flux on outlet mass flow at no induced wind, CH of 5 m and SHF of 400 W/m$^2$ condition for Ra = $10^{12}$ – $10^{14}$.

## Results and discussions

### *Model validation*

The model was validated with experimental results of effect of heat flux on the air flow rate from Chen et al. [13] (Fig. 3) and simulated results of mass flow rate from Miyazaki et al. [30] (Fig. 2). The present study shows a good agreement with results found in literature for CFD and experimental studies [13,30] with a deviation of 2.5% with the experimental results of Chen et al. [13] while the deviation from the simulated results of Miyazaki et al. [30] was found to be about 7.4%.

### *Effect of solar heat flux (SHF), chimney height and gap on mass flow rate*

The outlet mass flow was observed to increase from 0.5 to 0.8 kg/s (Ra = $10^{14}$) for SHF of 200 and 1 000 W/m$^2$ respectively (Fig. 4), with chimney height of 5 m and gap of 1 m. When the chimney height was increased from 5 – 9 m (Ra = $10^{14}$) with gap of 1 m and SHF of 400 W/m$^2$, the mass flow was also observed to have increased from 0.5 – 0.8 kg/s respectively (Fig. 5). The mass flow rate of 0.6 and 0.9 kg/s was observed for gap of 0.5 and 1.0 m respectively (Fig. 6), with chimney height of 9 m and SHF of 400 W/m$^2$. This observation confirms results from literature that the chimney height is the major factor in determining the power output and ventilation rate of the SC [24,37,40,44].

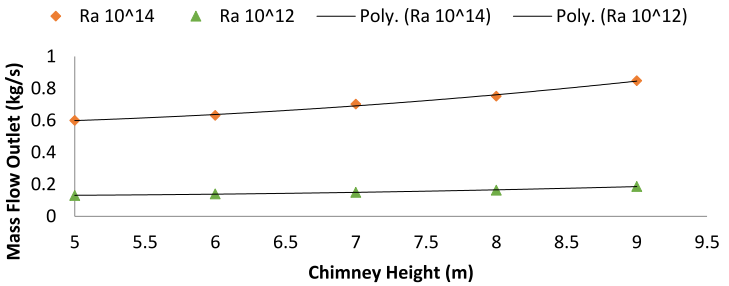


**Fig. 5.** Effect of chimney height on mass flow at outlet at no induced wind, CH of 5 m and SHF of 400 W/m$^2$ condition for Ra = $10^{12}$ – $10^{14}$.

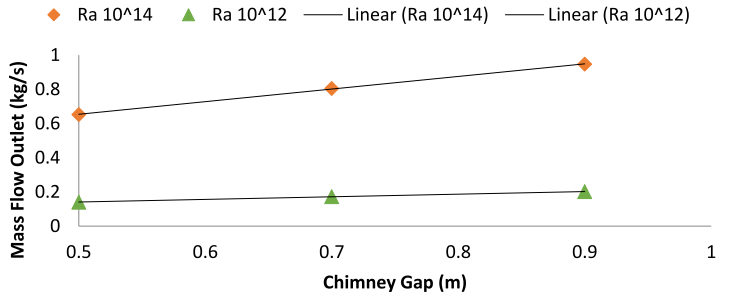


**Fig. 6.** Effect of chimney gap on outlet mass flow at no induced wind, CH of 5 m and SHF of 400 W/m$^2$ condition for Ra = $10^{12}$ – $10^{14}$.

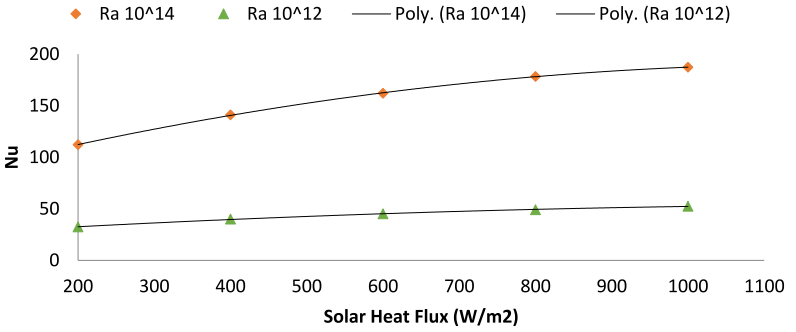


**Fig. 7.** The effect of solar heat flux on average Nusselt number at no induced wind, CH of 5 m and SHF of 400 W/m$^2$condition for Ra = $10^{12}$ – $10^{14}$.

*Effect of chimney height, chimney gap and solar heat flux on the Nusselt Number*

The effect of chimney height, chimney gap and solar heat flux on the Nusselt number (Nu) on the vertical solar collector (chimney) at Ra = $10^{12}$ to $10^{14}$ were simulated on a 2D model. It was observed that an increase in chimney height, chimney gap and the solar heat flux increased the average surface Nu as expected from theory (Figs. 7–9). It was further observed that a combined effect of both the SHF and the induced wind velocity resulted in a further increase in Nu. The effect of the SHF of 1,000 W/m$^2$ with an induced wind of 1 m/s resulted in Nu of about 450, while the same solar heat flux of 1,000 W/m$^2$ and wind of 0.05 m/s produced Nu of about 150, which was a 200% increase in Nu with wind aided SC.

The chimney height of 5 m and 9 m resulted in a net Nu on both walls of 180.66 and 194.07 (Ra = $10^{14}$) respectively, with a difference of 13.41. This inferred that the convective heat transfer phenomenon was more relevant than the conductive heat transfer phenomenon for this case. This implies that a change in the height of the chimney from 5 m to 9 m improved the heat transfer rate by about 7%. Moreover, at lower Ra the effect of conduction become noticeable.

The chimney gap of 0.5 m and 1.0 m produced a net Nu on both walls of 170.99 and 189.49 (Ra = $10^{14}$) having a difference of 18.5. It was observed, from the results obtained that a chimney width/ height combination that maximised the heat transfer rate were found to be 0.5 m/ 7 m and 1 m/ 5 m.

*Effect of solar heat flux, chimney height and flow velocity on power output*

The flow power output per unit area increased by 56.4% from 39 – 61 W/m$^2$ for SHF of 200 and 1,000 W/m$^2$ (Ra = $10^{14}$) respectively (Fig. 11), which gave a SHF to flow power conversion of 19.5 % and 6.1 % at SHF of 200 and 1,000 W/m$^2$

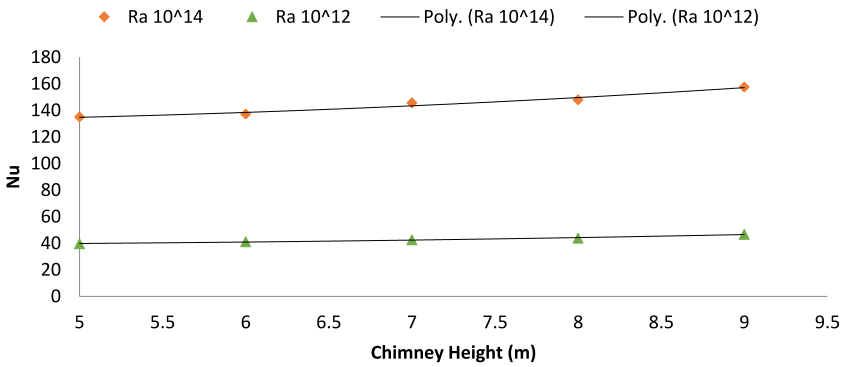


**Fig. 8.** Effect of chimney height on nusselt number at no induced wind, CH of 5 m and SHF of 400 W/m$^2$condition for Ra = $10^{12}$ – $10^{14}$.

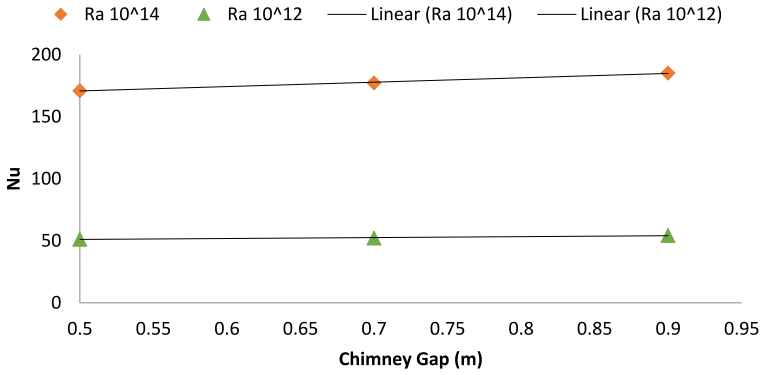


**Fig. 9.** Effect of chimney gap on the average surface Nusselt number with no induced wind, CH of 5 m and SHF of 400 W/m$^2$

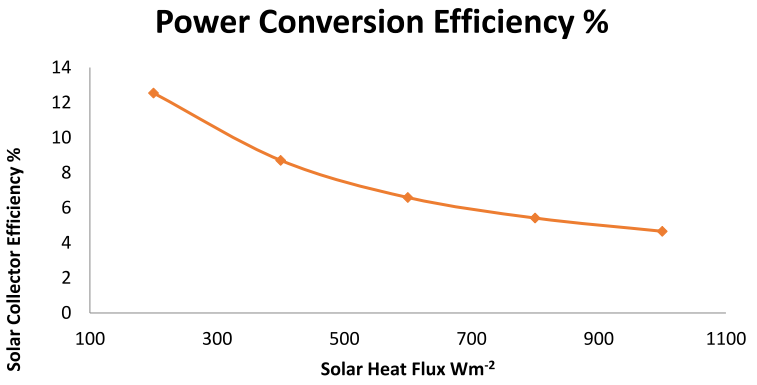


**Fig. 10.** Solar collector efficiency with increase in solar heat flux.

respectively (Fig. 10). This implies that as the flux increases the flow power conversion reduces, which is attributed to the system's fixed configuration. Other means of extracting power must be sought as this happens. Furthermore, the effect of a buildup of heat energy in the collector has not been accounted for in the present steady state analysis, and this heat buildup will affect the channel flow velocity and invariably the flow power output. A transient analysis will conversely reveal an improved conversion efficiency where the temperature difference would increase over time as the channel is being heated up. The effect of the chimney height on the flow power output of the SC was a 154.6 % increase from a flow power output of 44 – 112 W/m$^2$ at chimney height of 5 and 9 m respectively (Fig. 12) at solar heat flux of 400 W/m$^2$ (Ra = $10^{14}$). The conversion effect (ratio of flow power to chimney height) of 8.8 and 12.4 were estimated for chimney heights of 5 and 9 m respectively.

The flow velocity is an important factor for determining the output power of the SC. Results showed that an increase in channel velocity from 0.05 – 1.5 m/s caused the power output to increase from about 3.1 – 92.1 W/m$^2$, while an increase

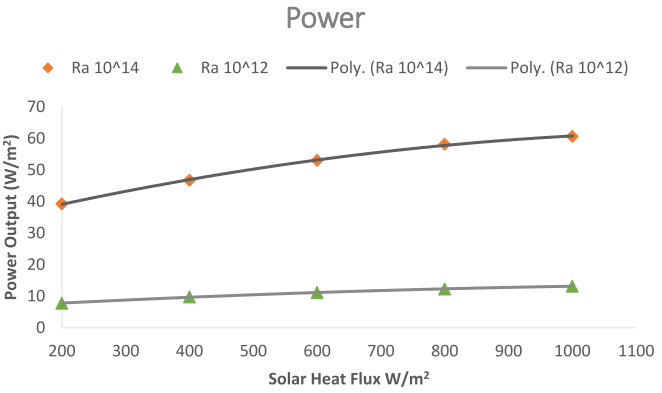


**Fig. 11.** Effect of solar heat flux on power output for Ra = $10^{12}$ - $10^{14}$.

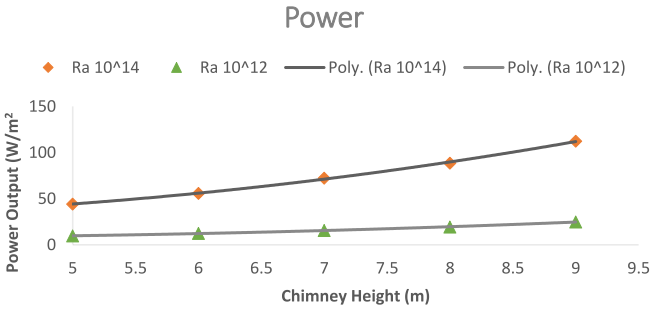


**Fig. 12.** Effect of Chimney Height on Power Output for Ra = $10^{12}$ - $10^{14}$

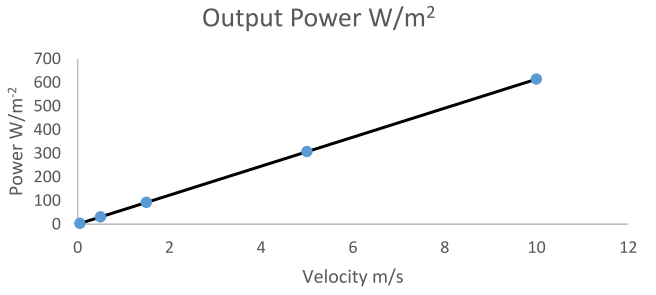


**Fig. 13.** Effect of chimney flow velocity on power output.

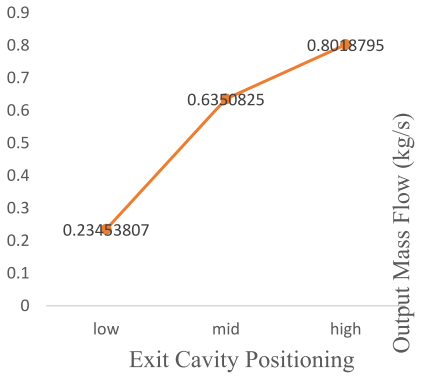


**Fig. 14.** The effect of exit cavity positioning on output mass flow.

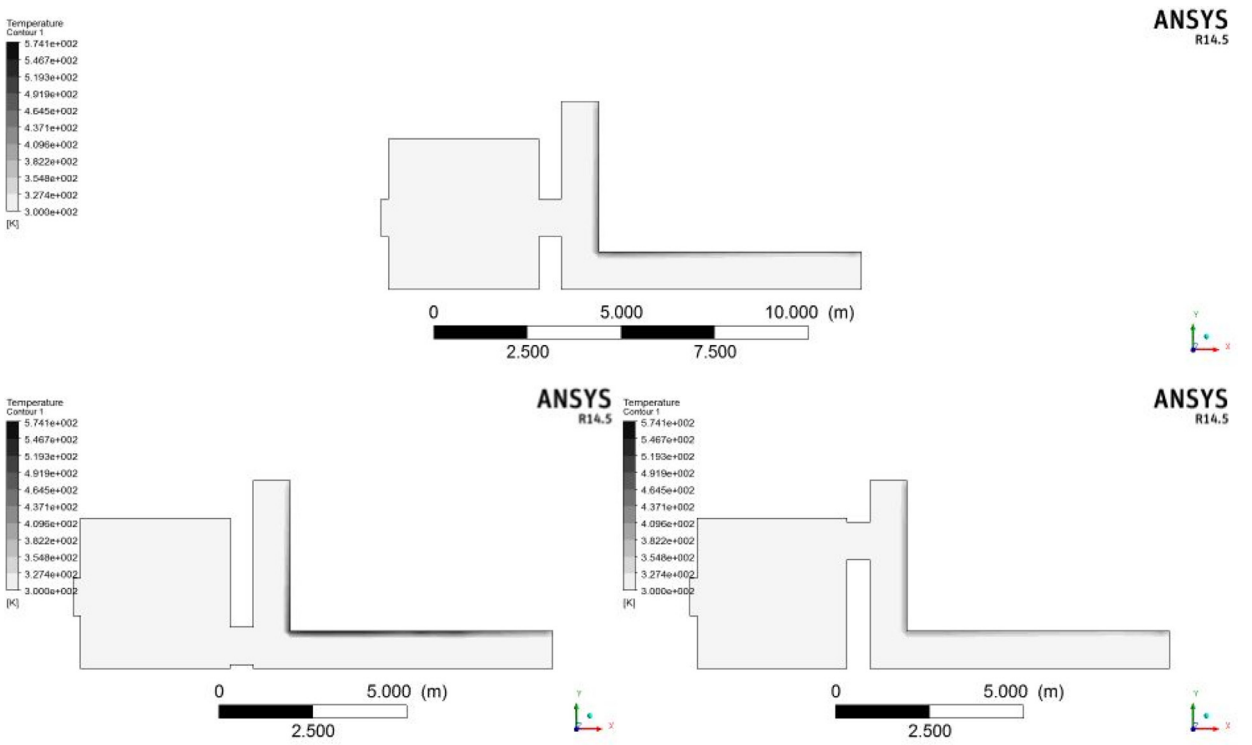


**Fig. 15.** Temperature contours of the high, mid and low exit cavity positioning showing the temperature distribution comparison at no induced wind, CH of 5 m and SHF of 400 W/m$^2$

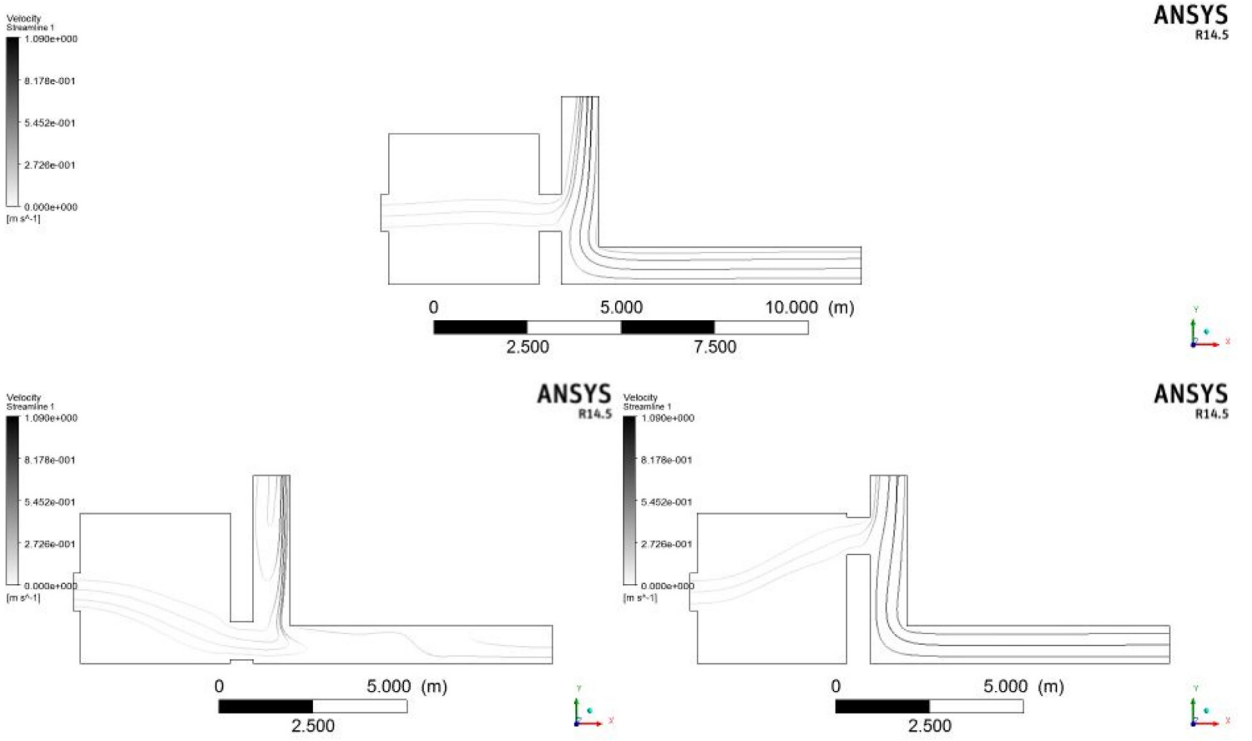


**Fig. 16.** Streamlines of the high, mid and low exit cavity positioning showing the flow comparison at no induced wind, CH of 5 m and SHF of 400 W/m$^2$.

from 5 to 10 m/s resulted in a power output of 307.1 and 614.1 W/m$^2$ respectively (Fig. 13). It is noted that the channel velocity was affected by factors, which include the ambient wind velocity, the temperature difference between the ambient temperature and the channel temperature (which are invariably due of the ambient solar radiation) and the geometry of the system. However, the factor within human control, being system's geometry, are important factors for the design of the dual purpose solar chimney. At constant ambient conditions, a convergent divergent channel (venturi effect) may help in increasing the velocity at required points for an increase in power output instead of the rectangular channel that was used.

*Effect of cavity position on the temperature distribution and outlet mass flow*

The effect of repositioning the exit cavity from low to high position showed outlet mass flow increased from 0.23 to 0.8 kg/s with SC of chimney height of 5 m, collector breadth of 1 m and SHF of 400 W/m$^2$. This showed that the top of the room is the best position for the exit cavity (Figs. 14–16).

The streamlines (Fig. 16), showing air movement, revealed that the top cavity position had the highest air movement of the three positioning considered. The streamlines for the centre cavity positioning however, is a cross flow with higher velocity at the centre of the room. Even distribution of flow above and below the cross flow section is also observed. However, slight presence of rotational flow at the top of the chimney, which caused a reduction in the mass flow at the chimney exit was also observed. The streamlines obtained from the low positioning of the cavity had longer swirling section starting from the chimney exit all the way down to a distance near the cavity inlet into the chimney. This reduced greatly the mass flow at the exit of the chimney. The horizontal solar collector region also showed swirling at the inlet and at upper sections for the case of low cavity positioning. This is as a result of the opposing flow from the room into the chimney.

The temperature (Fig. 15) gradient within the room for all the three cavity positioning showed similar and uniform distribution of temperature within the room. The effect of repositioning the exit cavity from low to high position showed that outlet mass flow increased from 0.23 to 0.8 kg/s with chimney height of 5 m, collector breadth of 1 m and SHF of 400 W/m$^2$. This showed that the top of the room is the best position for the exit cavity for power generation with the turbine placed at the top of the chimney.

## Conclusions

CFD analysis of a novel dual purpose solar chimney for both ventilation and power generation have been analysed and validated using existing CFD results and experimental data. The application of the proposed solar chimney system would be a very good solution the problem of ventilation (thermal comfort) and energy management (inadequate power supply) of buildings in the tropics. The main objective of the study was to determine the feasibility of the proposed system vis-à-vis the airflow rate within the room for adequate ventilation and within the solar chimney for required velocity to power a small size wind turbine. The climatic condition is as in South-west Nigeria, with ambient average temperature of 27 °C, mean air velocity of 1.2 m/s, atmospheric pressure of 1013mb, and the mean solar radiation of about 200 W/m$^2$. The commercial CFD package ANSYS FLUENT was used for the simulation. The analysis domain consist of a 2-D 4 $\times$ 4 m$^2$ room and L-shaped solar chimney with chimney heights varying from 5 to 9 m and gap from 0.5 to 1 m. The boundary conditions consist of the solar radiation with solar heat flux (SHF) between 200 and 1,000 W/m$^2$ and ambient wind conditions of no wind and wind speed of 1.0 to 8.0 m/s. It was found that positioning the exit cavity at ceiling level produced the highest exit mass flow rate. However, the cross ventilation positioning was better for the living area of the room. It was observed also that the room temperature has been maintained fairly at 27°*C* even with increase in solar heat flux. Observations also revealed that the room mass flow rate increased from 5.70 to 9.12 kg/s at chimney height of 5 and 9 m respectively at solar heat flux of 400 W/m$^2$. An increase in the chimney height was observed to improve the ventilation rate and power output of the system. The power output also increased with increased with increasing solar heat flux. The power outputs obtained from the SC with SHF of 400 W/m$^2$ for chimney height of 5 and 9 m were 32.8 and 85.2 W/m$^2$ respectively. The respective power output for SHF of 200 and 1,000 W/m$^2$ were 25.09 and 46.55 W/m$^2$ at CH of 5 m. The results presented helps layout and establish the fundamentals and system response to temperature and airflow of a solar chimney system used for the combined purpose of passive ventilation and power generation in a building.

This study recommends for further research:

1. A transient analysis which will reveal the relationship(s) of the performance characteristic of the combined ventilation and power SC with respect time if any.
2. Analysis based on other window positioning
3. Investigation into the performance of the "Ventapower" solar chimney using various collector materials and sizes is recommended.

## Declaration of competing interest

No conflict of interest is applicable to this work.

## References


[1] ANSYS FLUENT Theory Guide (2011) ANSYS, Inc., Southpointe, 275 Technology Drive, Canonsburg, PA 15317, ansysinfo@ansys.com, http://www.ansys.com, Release 14.0 November 2011.
[2] H. Awbi, G. Gan, Simulation of solar-induced ventilation, Renew. Energy Technol. Environ. 4 (1992) 16–30.
[3] E. Bacharoudis, M. Vrachopoulos, M. Koukou, D Margaris, A. Filios, et al. Study of the natural convection phenomena inside a wall solar chimney with one wall adiabatic and one wall under a heat flux, in: Applied Thermal Engineering, 27, Elsevier, 2007, p. 2266.
[4] N. Bansal, J. Mathur, M. Bhandari, Solar chimney for enhanced stack ventilation, Build. Environ. 28 (1993) 373–377.
[5] G. Barozzi, M. Imbabi, et al. Physical and numerical modelling of a solar chimney-based ventilation system for buildings, Build. Environ. 27 (1992) 33–45.
[6] A. Bar-Cohen, A. Krauss, Advances in Thermal Modeling of Electronic Components and Systems, Hemisphere Publishing Corporation, New York, 1988.
[7] R. Bassiouny, N. Korah, Effect of solar chimney inclination angle on space flow pattern and ventilation rate, Energy Build. 41 (2) (2009) 190–196.
[8] R. Bassiouny, N. Koura, An analytical and numerical study of solar chimney use for room natural ventilation, Energy Build. 40 (5) (2008) 865–873.
[9] E. Bilgen, J. Michel, Plenum Press, New York, 1979, pp. 279–296.
[10] A. Bouchair, Solar chimney for promoting cooling ventilation in southern Algeria, Build. Serv. Eng. Res. Technol. 15 (1994) 81–93.
[11] A. Bouchair, D. Fitzgerald, J. Tinker, Moving air using stored solar energy, in: Proceedings of the 13th National Passive Solar Conference Cambridge, 1988, pp. 8–33.
[12] Z. Chen, Y. Li, A numerical study of a solar chimney with uniform wall heat flux, in: Proceedings of the Fourth International Conference on Indoor Air Quality, Ventilation and Energy Conservation in Buildings, Hunan China, 2001, pp. 1447–1454.
[13] Z. Chen, P. Bandopadhayay, J. Halldorsson, C. Byrjalsen, P. Heiselberg, Y. Li, An experimental investigation of a solar chimney model with uniform wall heat flux, Build. Environ. 38 (2003) 893–906.
[14] O. Ekechukwa, B. Norton, Review of solar energy drying system II. An overview of solar drying technology, Energy Convers. Manage. 40 (1999) 615–655.
[15] T. Fluri, J. Pretorius, C. Van Dyk, T. Von Backstrom, D. Kroger, G. Van Zijl, Cost Analysis Of Solar Chimney Power Plants, Sol. Energy 83 (2009) 246–256.
[16] G. Gan, A parametric study of trombe walls for passive cooling of buildings, Energy Build. 27 (1998) 37–43.
[17] G. Gan, General expressions for the calculation of air flow and heat transfer rates in tall ventilation cavities, Build. Environ. 46 (10) (2011) 2069–2080.
[18] G. Gan, S. Riffat, A numerical study of solar chimney for natural ventilation of buildings with heat recovery, Appl. Therm. Eng. 18 (1998) 1171–1187.
[19] B. Hughes, S. Ghani, A numerical investigation into the feasibility of a passive-assisted natural ventilation stack device, Int. J. Sustainable Energy 30 (4) (2011) 193–211.
[20] C. Ikhile, The Impact of Climate Change on the Discharge of Osse-Ossiomo River Basin, South Western Nigeria under Different Climatic Scenarios, in: International Journal of Science and Technology, Bahir Dar, Ethiopia, 1, 2012, pp. 208–220.
[21] R. Khanal, C. Lei, Solar chimney—A passive strategy for natural ventilation, Energy Build. 43 (2011) 1811–1819.
[22] J. Khedari, B. Boonsri, J. Hirunlabh, Ventilation impact of a solar chimney on indoor temperature fluctuation and air change in a school building, Energy Build. 32 (2000) 89–93.
[23] S. Lal, S. Kaushik, P. Bhargava, A study on stack ventilation system and integrated approaches, Conference on Emerging Trends of Energy Conservation in Buildings, 1-3, 2012 255–263.
[24] W. Liu, T. Ming, K. Yang, Simulation of Characteristics of Heat Transfer and Flow for MW Grade Solar Chimney Power Plant, in: Proceedings of ISEC 2005, 2005 International Solar Energy Conference, Orlando, Florida, 2005 August 6-12, 2005ISEC2005-76221.
[25] A. Layeni, M. Waheed, O. Jeje, S. Giwa, Computational Analysis of a Dual Purpose Solar Chimney for Buildings in Nigeria, in: Proceedings of the 8th International Conference on Sustainable Energy & Environmental Protection (SEEP2015), 8, Paisley, 2015, pp. 363–369. August 11-14, 2015Pages.
[26] W. Lipping, L. Angui, A numerical study of vertical solar chimney for enhancing stack ventilation in buildings, in: The 21th Conference on Passive and Low Energy Architecture, Eindhoven, Netherlands, 2004, pp. 1–5. 2004.
[27] M. Maerefat, A. Haghighi, Natural cooling of stand-alone houses using solar chimney and evaporative cooling cavity, Renew. Energy 35 (2010) 2040–2052.
[28] J. Mathur, N. Bansal, S. Mathur, M. Jain, Anupma, Experimental investigations on solar chimney for room ventilation, Sol. Energy 80 (2006) 927–935.
[29] T. Ming, W. Liu, G. Xu, Analytical and numerical investigation of the solar chimney power plant systems, Int. J. Energy Recourses 30 (2006) 861–873.
[30] T. Miyazaki, A. Akisawa, T. Kashiwagi, The Effects of Sola Chimneys on Thermal Load Mitigation of Office Buildings under the Japanese Climate, Renew. Energy 31 (2006) 987–1010.
[31] H. Nouanegue, L. Alandji, E. Bilgen, Numerical study of solar-wind tower systems for ventilation of dwellings, Renew. Energy 33 (2008) 434–443 2008.
[32] H. Nouanégué, E. Bilgen, Heat transfer by convection, conduction and radiation in solar chimney systems for ventilation of dwellings, Int. J. Heat Fluid Flow 30 (2009) 150–157.
[33] P. Nwofe, Utilization of solar and biomas energy - A panacea to energy sustainability in a developing economy, Int. J. Energy Environ. Res. 2 (3) (2014) 10–19.
[34] K. Ong, A mathematical model of a solar chimney, Renew. Energy 28 (2003) 1047–1060.
[35] K. Ong, C. Chow, Performance of a solar chimney, Sol. Energy 74 (2003) 1–17.
[36] A. Peri, P. Fernandes, C. Vishwanadha, Numerical Simulation of Air Flow in a General Ward of a Hospital, Int. J. Res. Rev. Appl. Sci. 8 (3) (2011).
[37] J. Pretorius, D. Kröger, Critical evaluation of solar chimney power plant performance, Sol. Energy 80 (2006) 535–544.
[38] J. Pretorius, Optimization and Control of a Large-scale Solar Chimney Power Plant, Dissertation presented for the degree of Doctor of Mechanical Engineering at the University of Stellenbosch, 2007.
[39] J. Pretorius, D. Kröger, The Influence of Environment on Solar Chimney Power Plant Performance, R & D J. South Afr. Inst. Mech. Eng. 25 (2009) http://www.saimeche.org.za. (open access).
[40] J. Schlaich, W. Schiel, Solar Chimneys, Encyclopedia of Physical Science and Technology, Schlaich Bergermann und Partner, Consulting Engineers, Stuttgart, Third Edition 2000, 2000 http://citeseerx.ist.psu.edu/viewdoc/download?doi=10.1.1.454.1346&rep=rep1&type=pdf (Viewed 1st November 2012, 1st October 2015).
[41] L. Zalewski, S. Lassue, B. Duthoit, M. Butez, Study of solar walls- validating a numerical simulation model, Int. Rev. Build. Environ. 37 (2002) 109–121 2002.
[42] B. Zamora, A. Kaiser, Optimum wall-to-wall spacing in solar chimney shaped channels in natural convection by numerical investigation, Appl. Therm. Eng. 29 (4) (2009) 762–769.
[43] X. Zhou, J. Yang, B. Xiao, G. Hou, F. Xing, Analysis of chimney height for solar chimney power plant, Appl. Therm. Eng. 29 (2009) 178–185.
[44] X. Zhou, J. Yang, F. Wang, B. Xiao, Economic analysis of power generation from floating solar chimney power plant, Renew. Sustainable Energy Rev. 13 (2009) 736–749.
[45] X. Zhou, F. Wanga, R.M. Ochieng, A review of solar chimney power technology, Renew. Sustain. Energy Rev. 14 (2010) 2315–2338.